Monthly Notices of the ROYAL ASTRONOMICAL SOCIETY

MNRAS **525,** 1929–1935 (2023) https://doi.org/10.1093/mnras/stad2372
Advance Access publication 2023 August 3

Stability of hierarchical triples – II. The inclination $\iota = 140°$ resonance in the stability surface

Alexey Pasechnik,[1,2]★ Aleksandr Mylläri,[3,4]★ Mauri Valtonen[1,5] and Seppo Mikkola[1]

[1]*Tuorla Observatory, Department of Physics and Astronomy, University of Turku, FI-20014 Turku, Finland*
[2]*EPAM Sistemos, UAB, Šeimyniškiu g. 19-601, LT-09236 Vilnius, Lithuania*
[3]*Department of Mathematics, Åbo Akademi University, Tuomiokirkontori 1, FI-20500 Turku/Åbo, Finland*
[4]*School of Arts and Sciences, St. George's University, St. George's, Grenada, West Indies*
[5]*Finnish Centre for Astronomy with ESO (FINCA), University of Turku, FI-20014 Turku, Finland*

Accepted 2023 July 26. Received 2023 July 21; in original form 2022 January 8

ABSTRACT

The stability of a hierarchical triple star may be decided by a simple criterion, which was derived in Paper I. However, there is a region in the phase space where the stability limit $Q_{\rm max}$ is raised by a factor of two in a small region of the phase space with respect to the surrounding phase space. The phase space is defined by the inner and outer eccentricities $e_{\rm in}$ and $e_{\rm out}$, respectively, as well as by the inclination $\iota_{\rm tot}$ between the inner and outer orbits. Additional parameters of the phase space are the masses of the three bodies. We study by numerical integration the orbits of over 100 000 triple systems in the resonance region. We find that the instability that causes the high value of $Q_{\rm max}$ arises from the octupole Kozai–Lidov resonance. This resonance region has rather equal contributions from the quadrupole and octupole terms and leads to secular evolution with an amplitude larger than either of the two oscillations in isolation. The conditions for this situation are best satisfied near the relative inclination $\iota = 140°$. Additionally, the relative orientation of the two orbits plays a decisive role: the resonance is found only at certain values of the orbit's node line longitude Ω. An analytical approximation of the energy change in a single close encounter between the inner and outer systems suggests a $\cos 2\Omega$ dependence of $Q_{\rm max}$ on Ω, which seems to be qualitatively valid. We model $Q_{\rm max}$ as a function of $\cos\iota$ and $e_{\rm in}$ by a Gaussian function.

Key words: methods: numerical – celestial mechanics.

1 INTRODUCTION

Hierarchical triple structures are common in many systems in the Universe. We consider structures where two bodies move around each other under Newton's law of gravity while, at the same time, a third body moves around the binary centre of mass under the same force law. The initial state may be described by 15 parameters: six orbital elements of the binary and six elements of the third body motion relative to the binary. In addition, three masses are to be specified. By scaling, we may reduce the problem to 10 dimensions, but still the initial value space remains large even with a coarse sampling. Non-hierarchical case is considered, e.g. in Zhang, Naoz & Will (2023).

For each initial state, it is possible to carry out an orbital integration and discover the future evolution of the triple system. One of the questions we may ask is whether the system is stable in the sense that the third body remains bound to the binary over a given length of time, preferably measured in natural units of the system (Harrington 1968, 1969, 1972, 1975, 1977; Nacozy 1976; Szebehely 1976; ; Szebehely & McKenzie 1977; Szebehely & Zare 1977; Aarseth 2003; Heggie & Hut 2003; Valtonen & Karttunen 2006). In this paper, we will consider 10 000 outer revolutions of the third body in its initial orbit. Instability may also lead to the exchange of one of the inner binary members with the third body. Here, we will consider the instability defined by either of these two outcomes of the orbital evolution. The third possibility is the physical collision of two bodies when they have finite sizes, as is always the case in nature.

It is common in stability studies to divide the orbital elements into three categories: the important ones, such as the mass values; the less important ones, such as the angular variables $\omega_{\rm in}$, $\omega_{\rm out}$ (arguments of the perihelion of the inner and outer orbits, respectively), and Ω (longitude of ascending node of the outer orbit); and the fixed ones. The initial binary plane may be taken as the fundamental plane, which means that the binary inclination and ascending node are zero by definition. Thus, our angular elements are ι (the relative orbital inclination), $\omega_{\rm in}$, $\omega_{\rm out}$, and Ω. Also, we may choose the origin of time such that the third body is in a given phase at the initial time, e.g. at the apocenter of its motion. Thus, three of the orbital elements are not free parameters. The fourth fixed parameter is the mass scale, which is freely chosen without affecting the qualitative results; alternatively, we may consider the time-scale as the free parameter.

Therefore, in our problem, we choose two of the masses. Here, we fix the binary total mass to two mass units and specify m_1, the heavier binary mass, and m_3, the third body mass. The physical scale is a free choice; we choose the binary semimajor axis as one unit and measure the semimajor axis of the third body $a_{\rm out}$ relative to it. This is our fifth fixed parameter, which leaves 10 free parameters. The six important

★ E-mail: alexey.pasechnik@gmail.com (AP); amyllari@gmail.com (AM)

parameters are the two mass values; the third body elements $a_{\rm out}$, ι; the outer eccentricity $e_{\rm out}$; and the inner eccentricity $e_{\rm in}$. The perihelion distance $Q = a_{\rm out}(1 - e_{\rm out})$. In fact, in the following, we will use $e_{\rm out}$ and Q as the important elements of the third body orbit.

The initial phase of the binary nt_0, the orientation of its major axis $\omega_{\rm in}$, and the third body elements $\omega_{\rm out}$ and Ω are generally treated as the less important ones. Here, n specifies the mean angular motion of the binary, which is unity by our definition. Thus, t_0 is the final and tenth free orbital element.

The traditional way to specify the stability limit problem is as follows: define $Q_{\rm max}$ as the largest possible Q that leads to an instability within a given interval of time. Here, $Q_{\rm max}$ is to be specified as a function of m_1, m_3, $e_{\rm in}$, $e_{\rm out}$, and ι while t_0, $\omega_{\rm in}$, $\omega_{\rm out}$, and Ω can take any values (Graziani & Black 1981; Walker & Roy 1981; Huang & Innanen 1983; Pendleton & Black 1983; Walker & Roy 1983; Donnison 1984; Roy et al. 1984; Dvorak 1986; Benest 1988; Donnison 1988; Rabl & Dvorak 1988; Benest 1989; Dvorak, Froeschle & Froeschle 1989; Donnison & Mikulskis 1992; Donnison & Mikulskis 1994; Eggleton & Kiseleva 1995; Holman & Wiegert 1999; Mardling & Aarseth 1999; Pilat-Lohinger, Funk & Dvorak 2003; Valtonen & Karttunen 2006; Mardling 2008; Valtonen et al. 2008, see a review by Georgakarakos 2008).

In our Paper I (Mylläri et al. 2018), we derived a general solution to the problem, with one important exception. For inclinations near 140°, i.e. at approximately $\cos\iota = -3/4$, there is a narrow resonance region, where $Q_{\rm max}$ becomes about twice as large as at surrounding values of $\cos\iota$. This was already noticed by Valtonen et al. (2008), but no further studies were carried out. In previous work, no other resonances of this magnitude have come up. Thus, in this work, we concentrate on this particular region of the phase space.

2 ORBIT INTEGRATIONS

Most of the orbital integrations are carried out by a symplectic method, which has the property of conserving total energy (Mikkola 1997).

For comparison, we have integrated a smaller number of cases by a Hermitian integrator and by a three-body regularization code (Aarseth & Zare 1974).

Also, we calculated a number of cases by direct numerical solution of the Newtonian equations of motion in the Cartesian coordinate system using the Runge–Kutta–Fehlberg method – RK4(5) (Fehlberg 1969), with adjustable time-step. On each step, we calculate the maximum acceleration of any three bodies: $a_{\rm max} = \max(|\vec{a}_1|, |\vec{a}_2|, |\vec{a}_3|)$. Then the time-step for the next step is set to the value $h = v_{\rm p}/a_{\rm max}$, where $v_{\rm p}$ is an empirically defined parameter, its optimal value for the studied configuration lies between 0.5 and 2.0 km s^{-1}.

We found that the result is not integrator dependent.

Figs 1 and 2 illustrate the independence of the result from the integration method for the system with following initial parameters: $m_1 = 1.5\,{\rm M}_\odot$, $m_2 = m_3 = 0.5\,{\rm M}_\odot$, $e_{\rm in} = 0.6$, $e_{\rm out} = 0.5$, $\iota_{\rm tot} = 140°$, $\omega_{\rm in} = 60°$, $\omega_{\rm out} = 155°$, $a_{\rm in} = 1$ au, and $Q = 5$. Fig. 1 shows three tracks of the change in $\cos\iota_{\rm tot}$ over time, computed, respectively: the symplectic method (blue), the Runge–Kutta–Fehlberg method (red), and the Wolfram Mathematica 'StiffnessSwitching' (black). Fig. 2 shows the differences between the results of the symplectic method (blue) and the Runge–Kutta–Fehlberg (red) relative to the result of 'StiffnessSwitching' method. As we can see, all three methods predict the decay of the system near the region of 1200 revolutions of the external component, i.e. the key result we are interested in our investigations of the system stability.

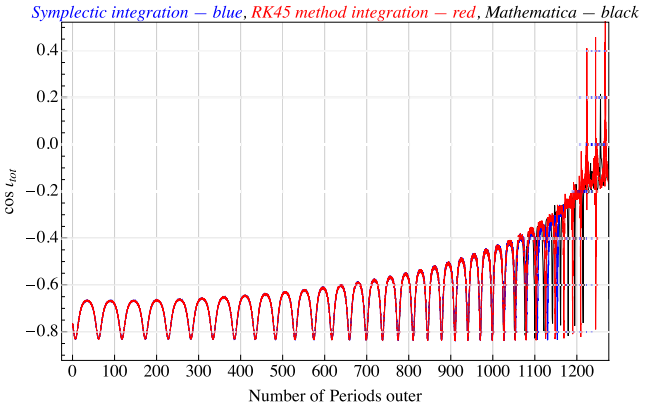

Figure 1. Evolution of the $\cos\iota_{\rm tot}$ calculated using the symplectic method (blue), the Runge–Kutta–Fehlberg method (red), and the 'StiffnessSwitching' (black) method for the system with initial parameters: $m_1 = 1.5\,{\rm M}_\odot$, $m_2 = m_3 = 0.5\,{\rm M}_\odot$, $e_{\rm in} = 0.6$, $e_{\rm out} = 0.5$, $\iota_{\rm tot} = 140°$, $\omega_{\rm in} = 60°$, $\omega_{\rm out} = 155°$, $a_{\rm in} = 1$ au, and $Q = 5$.

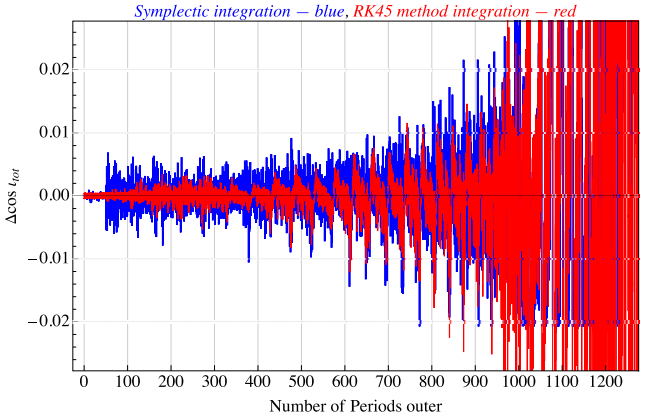

Figure 2. The differences between the results of the symplectic method (blue) and the Runge–Kutta–Fehlberg (red) relative to the result of 'StiffnessSwitching' method.

Initially, we used the following method to determine the maximum parameter Q of system stability: the value of Q is first set so high that the system is stable for $N = 10\,000$ revolutions. Then, in a series of subsequent simulations, the value of Q is decreased in steps of 0.1 until we find instability. However, this approach has several disadvantages. First, the choice of the initial maximum value of Q was arbitrary, and second, often an overestimated value was chosen, which led to a very long computation time, namely, testing of all stable values of Q until the first instability was obtained.

Therefore, the method for finding the maximum unstable Q was subsequently changed. The calculation began with the value $Q = 1$, a guaranteed unstable configuration, and then the value of Q was increased by step 0.1 until 10 stable configurations in a row were found. The first stable value of Q in this series was taken as the $Q_{\rm max}$ corresponding to a stable configuration. Numerous comparisons of this method with the one previously used on various configurations of the triple system were carried out, and no cases were found when the modified method would give a wrong result.

The process is repeated for 100 values of $\cos\iota$ and for 50 values of Ω. A two-dimensional diagram of Q versus $\cos\iota$ and Ω is generated for several values of eccentricity in the region of $e_{\rm in} = 0.6$. In this diagram, the $Q_{\rm max}$ versus $\cos\iota$ and Ω surface is identified and is called

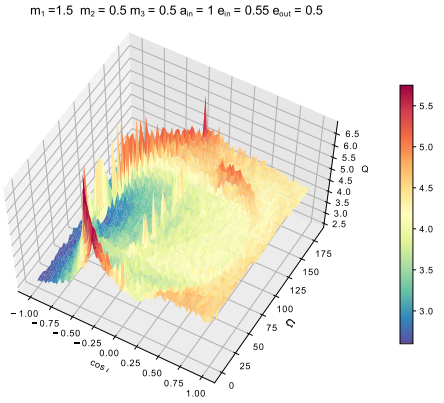

Figure 3. $Q_{\max}$ versus $\cos\iota$ and Ω surface for value $e_{\rm in} = 0.55$, $m_1 = 1.5\,{\rm M}_\odot$, $m_2 = m_3 = 0.5\,{\rm M}_\odot$, $a_{\rm in} = 1$ au, $e_{\rm out} = 0.5$.

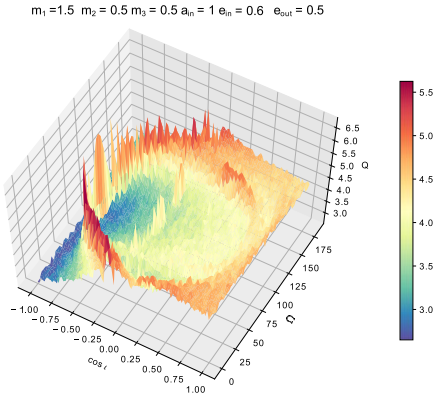

Figure 4. $Q_{\max}$ versus $\cos\iota$ and Ω surface for value $e_{\rm in} = 0.60$, $m_1 = 1.5\,{\rm M}_\odot$, $m_2 = m_3 = 0.5\,{\rm M}_\odot$, $a_{\rm in} = 1$ au, $e_{\rm out} = 0.5$.

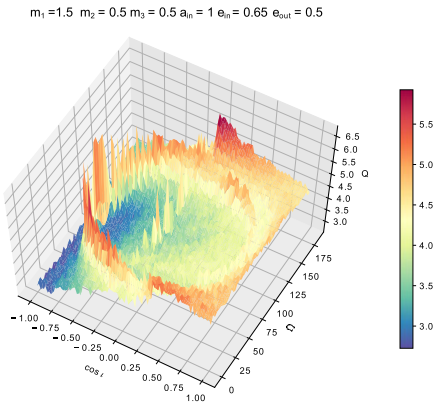

Figure 5. $Q_{\max}$ versus $\cos\iota$ and Ω surface for value $e_{\rm in} = 0.65$, $m_1 = 1.5\,{\rm M}_\odot$, $m_2 = m_3 = 0.5\,{\rm M}_\odot$, $a_{\rm in} = 1$ au, $e_{\rm out} = 0.5$.

the stability surface. It is always wiggly, as it samples the instability layer with fixed values of the 'less-essential' orbital elements. Then a new value of $e_{\rm in}$ is selected, and a new diagram is generated.

Figs 3, 4, and 5 show the $Q_{\max}$ versus $\cos\iota$ and Ω surface for three values $e_{\rm in} = 0.55$, 0.6, and 0.65. Other parameters are: $m_1 = 1.5\,{\rm M}_\odot$, $m_2 = m_3 = 0.5\,{\rm M}_\odot$, and $e_{\rm out} = 0.5$. Qualitatively, the behaviour is the same: $Q_{\max}$ depends on the orbital phase with respect to the 2Ω angle, i.e. in a doubly periodic manner.

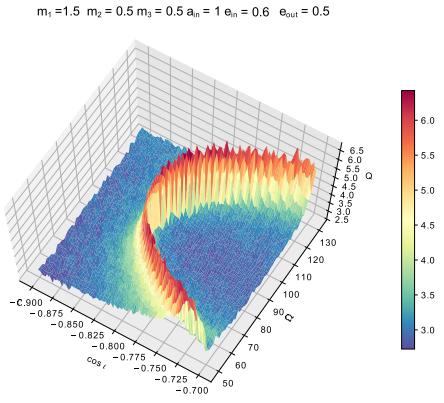

Figure 6. $Q_{\max}$ versus $\cos\iota$ and Ω surface for value $e_{\rm in} = 0.6$, $\iota = 134°$–$154°$, $\Omega = 50°$–$130°$, $m_1 = 1.5\,{\rm M}_\odot$, $m_2 = m_3 = 0.5\,{\rm M}_\odot$, $a_{\rm in} = 1$ au, $e_{\rm out} = 0.5$.

The 'jagged mountain range' effect on the diagram is a computational artefact associated with a discrete set of parameters $\cos\iota$ and Ω. To verify this, we carried out a series of simulations with a smaller step of changing the initial parameters. Fig. 6 shows the area within which we changed the $\cos\iota$ in the range from -0.9 to -0.7 (which corresponds to angles from 134° to 154°) with a step of 0.002 and Ω in the range from 50° to 130° with a step of 1.6°. Here, the distance between the peaks is smaller; it corresponds to the scale of the grid.

3 THEORY: RANDOM ENCOUNTERS

The theoretical understanding of these features requires results from two lines of research: what happens in a single encounter between the inner binary and the third body passing through its pericentre, and how the repeated encounters play out. Heggie and associates have worked on the first problem (Roy & Haddow 2003; Heggie 2006) and we use their results in the following. Another presentation of the problem is found in Valtonen & Karttunen (2006). Roy & Haddow (2003) calculate the energy change $\delta\varepsilon/\varepsilon$ of the binary in a single three-body encounter when the outer orbit is parabolic. Here, ε is the binary energy, and $\delta\varepsilon$ is the change arising from the encounter. The full expression is (with the leading terms of the Bessel functions inserted):

$$\begin{aligned}\frac{\delta\varepsilon}{\varepsilon} \simeq\ & 12\frac{m_3}{(m_1+m_2)}\frac{\sqrt{\pi}}{4}\left\{Q^{-3}K^{2.5}e^{-(2/3)K}\right\}e_{\rm in}\\ &\times\Big\{\Big[\left(1-4/9e_{\rm in}^2\right)\cos\iota+0.5\sqrt{1-e_{\rm in}^2}\left(1-5/36e_{\rm in}^2\right)\\ &\times\left(1+\cos\iota^2\right)\Big]\cos\left(2\omega_{\rm out}+nt_0\right)\sin d\Omega\\ &+\Big[\sqrt{1-e_{\rm in}^2}\left(1-5/36e_{\rm in}^2\right)\cos\iota+0.5\left(1-4/9e_{\rm in}^2\right)\\ &\times\left(1+\cos\iota^2\right)\Big]\sin\left(2\omega_{\rm out}+nt_0\right)\cos 2\Omega+1/3\left(1-1/8e_{\rm in}^2\right)\\ &\times\left(1-\cos\iota^2\right)\sin\left(2\omega_{\rm out}+nt_0\right).\end{aligned}$$

Here,

$$K = Q^{1.5}\sqrt{2\left(m_1+m_2\right)/\left(m_1+m_2+m_3\right)}$$

and ι, $\omega_{\rm out}$, and Ω are the inclination, the argument of the pericentre, and the longitude of the ascending node of the third body orbit relative to the binary centre. The mean motion of the binary is n and t_0 is the time since the third body pericentre passage. The quantity in the first curly brackets is well approximated by a factor proportional to

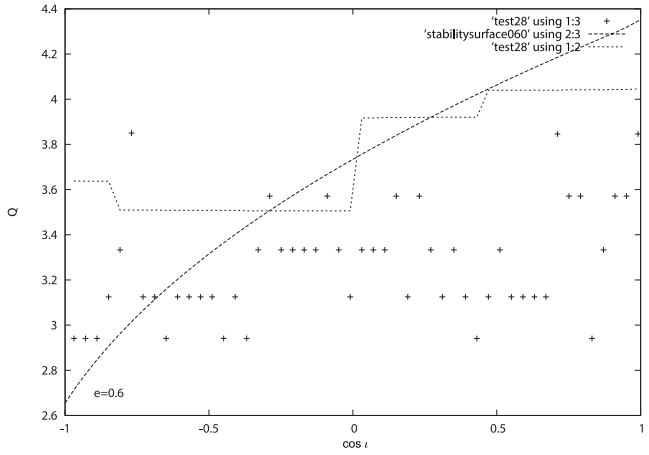

Figure 7. Stability limit based on the single encounter plus random energy evolutions.

$(Q/Q_1)^{-7}$, where

$$Q_1 = 2.5\,(1 + m_3/\,(m_1 + m_2))^{1/3}$$

(Valtonen & Karttunen 2006). Looking at the oscillating terms in the curly brackets, we generate a constructive interference by combining the first two terms: at zero eccentricity and at eccentricity approaching unity they have the same amplitude, while at intermediate eccentricities the amplitudes are not very different. This amplitude is generally higher than the amplitude of the third term and the related phase part is $\{\sin(2\omega_{\rm out} + nt_0 - 2\Omega)\}$ for retrograde orbits and $\{\sin(2\omega_{\rm out} + nt_0 + 2\Omega)\}$ for direct orbits. Thus,

$$\frac{\delta\varepsilon}{\varepsilon} \approx 0.1\frac{m_3}{(m_1+m_2)}\,(Q/Q_1)^{-7}\left(1 - 0.5e_{\rm in}^2\right) \times [1+\cos\iota]^2\{\sin\,(2\omega_{\rm out} + nt_0 \pm 2\Omega)\}.$$

The sinusoidal factor in curly brackets is phase dependent. Since we may assume that repeated encounters do not keep the phase, this factor causes a drift in energy space, which we may model by a random walk with the step size of the order of the amplitude of the phase factor.

By energy conservation, the relative energy change of the binary translates into the corresponding change in the outer orbit $\delta E/E$ (in the terminology of Mardling & Aarseth (2001), chaotic energy change):

$$\frac{\delta\varepsilon}{\varepsilon} \approx -\frac{m_3}{(m_1+m_2)}\,\frac{1-e_{\rm out}}{Q/Q_1}\,\frac{\delta E}{E}.$$

After N encounters, we expect the total energy to change by $\sqrt{N}\,\delta E$. When this amounts to E, we definitely have an unstable situation. We equate the amplitude of the first of the previous equations to the right-hand side of the second equation and solve for Q:

$$Q \approx 3.7(\sqrt{N})^{1/6}\left(1+\frac{m_3}{m_1+m_2}\right)^{1/3}\left(1-0.5e_{\rm in}^2\right)^{1/6} \times [1+\cos\iota]^{1/3}\,(1-e_{\rm out})^{-1/6}\,.$$

Note that typically the Q value increases going from retrograde orbits to direct orbits due to the similar property of the single orbit energy change. Actually, the inclination factor must be more complex than $[1+\cos\iota]^{1/3}$ as Q cannot go to zero at $\cos\iota = -1$. Fig. 7 illustrates the stability limit based on the single encounter plus random energy evolution (dashed line). The dotted line gives the corresponding curve in the Mardling (private communication) theory. The experimental points (crosses) lie well above either line at $\cos\iota \cong -3/4$. The other parameters are $m_1 = 1.5\,{\rm M}_\odot$, $m_3 = 0.5\,{\rm M}_\odot$, $e_{\rm in} = 0.6$, $e_{\rm out} = 0.5$. The Q values actually rise even higher at the resonance when the parameters are sampled more densely (Fig. 13).

4 THEORY: KOZAI–LIDOV RESONANCE

The Kozai–Lidov resonance (Kozai 1962; Lidov 1962) will affect $e_{\rm in}$ and $\cos\iota$ in a periodic manner (see, e.g. Mazeh & Shaham 1979; Valtonen & Karttunen 2006). The energy change $\delta\varepsilon/\varepsilon$ is practically independent of $e_{\rm in}$ but a strong function of $\cos\iota$. Thus, the Kozai cycle can move the system to a region in phase space where $\delta\varepsilon/\varepsilon$ is considerably greater than at the starting configuration. This process spreads high Q values to the left (to low $\cos\iota$) within the range where the Kozai cycle operates, from $\iota = 40^\circ$ to 140°. That is, Q versus $\cos\iota$ should be rather flat in this range.

The study of the individual resonance orbits shows that they arise from an inclination flip from negative $\cos\iota$ to positive $\cos\iota$. Since $\delta\varepsilon/\varepsilon$ is much greater at positive $\cos\iota$ than at negative $\cos\iota$, the high Q value may be 'transferred' from the positive side to the negative side. Such a process is not possible in the standard Kozai–Lidov theory. However, if the octupole terms are taken into account (Söderhjelm 1984; Marchal 1990; Krymolowsky & Mazeh 1999), we get a much richer variety of orbit possibilities (Ford, Kozinsky & Rasio 2000; Lithwick & Naoz 2011). Ford et al. (2000) note that the octupole terms dominate outside the standard Kozai–Lidov range, $\iota < 40^\circ$ and $\iota > 140^\circ$, but that their influence on the dynamical evolution of the triple is small. At the limit of $\iota = 40^\circ$ or 140°, the quadrupole and octupole effects are comparable and can lead to secular evolution with a period and amplitude larger than either of the two oscillations in isolation.

The evolution of the orbital elements of the inner and outer binaries has been described analytically by several authors (e.g. Naoz et al. 2013; Liu, Munoz & Lai 2015). The equation for the inner eccentricity reads

$$\frac{{\rm d}e_{\rm in}}{{\rm d}t} = \frac{\sqrt{1-e_{\rm in}^2}}{64t_{\rm K}}\big\{120e_{\rm in}\sin^2\iota\sin 2\omega_{\rm in} + 15\varepsilon_{\rm Oct}[\sin\omega_{\rm in}\cos\omega_{\rm out}\,[1] - \cos\omega_{\rm in}\sin\omega_{\rm out}\,[2]]\big\},$$

where

$$A = 4 + 3e_{\rm in}^2 - 105e_{\rm in}^2\sin^2\iota\sin^2\omega_{\rm in} - 15\left(1-e_{\rm in}^2\right)\sin^2\iota,$$
$$[1] = [A + 10\left(1+6e_{\rm in}^2\right)\sin^2\iota]$$
$$[2] = \cos\iota\,[A]\,,$$

the Kozai–Lidov time-scale is given by

$$t_{\rm K} = \frac{1}{n}\left(\frac{m_1+m_2}{m_3}\right)Q^3\left(1-e_{\rm out}^2\right)^{-3/2}$$

and the octupole coefficient is

$$\varepsilon_{\rm Oct} = \left(\frac{m_1-m_2}{m_1+m_2}\right)\frac{1}{Q}\left(\frac{e_{\rm out}}{1+e_{\rm out}}\right).$$

The factors [1] and [2] are different, except when ι is small. Then the last two factors combine to $15\varepsilon_{\rm Oct}\left(4+3e_{\rm in}^2\right)\sin(\omega_{\rm in}-\omega_{\rm out})$ and the quadrupole and the octupole terms may cancel each other when

$$\iota \cong \sqrt{\varepsilon_{\rm Oct}(\sin(\omega_{\rm out}-\omega_{\rm in})/\sin 2\omega_{\rm in})\left(4+3e_{\rm in}^2\right)/(8e_{\rm in})} \sim 10^\circ.$$

This is below the Kozai–Lidov inclination range, unless $\omega_{\rm in}$ is small. Then

$$120e_{\rm in}\sin^2\iota\,2\omega_{\rm in} \cong 15\varepsilon_{\rm Oct}\cos\iota \times\left[4+3e_{\rm in}^2 - 15\left(1-e_{\rm in}^2\right)\sin^2\iota\right]\sin\omega_{\rm out}.$$

At large eccentricity, $e_{\rm in} \simeq 1$

$$\cos\iota \simeq -\sqrt{z}(-1+\sqrt{1+1/z}),$$

where

$$z = \left[(7/16)\sin\omega_{\rm out}(\varepsilon_{\rm Oct}/2\omega_{\rm in})\right]^2.$$

Putting $\sin\omega_{\rm out} = 1/\sqrt{2}$ (its average value), $\varepsilon_{\rm Oct} \simeq 2\omega_{\rm in}$, and the eccentricity $e_{\rm in} \simeq 0.95$ gives $i \simeq 140^\circ$. At these inclinations, if it happens that $2\omega_{\rm in} \simeq \varepsilon_{\rm Oct}$ (which is likely from time to time since $\omega_{\rm in}$ circulates rapidly), then at the turning point of the inner eccentricity (when $\mathrm{d}e_{\rm in} \simeq 0$), $\mathrm{d}\iota/\mathrm{d}e_{\rm in}$ obtains a large value and the inclination may take a major hike in the $\cos\iota - e_{\rm in}$ plane. It can lead to a flip of $\cos\iota$ from the negative to the positive side, and to increased instability related to positive $\cos\iota$.

Also, the quadrupole and octupole terms may cancel when $\omega_{\rm in} \simeq \pi/2$:

$$120e_{\rm in}\sin^2\iota(\pi - 2\omega_{\rm in}) \cong -15\varepsilon_{\rm Oct}\left[4+3e_{\rm in}^2 - 5\left(1+6e_{\rm in}^2\right)\sin^2\iota\right]\cos\omega_{\rm out}.$$

We may solve for $\sin\iota$:

$$\sin^2\iota = \left(4+3e_{\rm in}^2\right)/\left(30e_{\rm in}^2+5-we_{\rm in}\right),$$

where

$$w = 8(\pi - 2\omega_{\rm in})/(\varepsilon_{\rm Oct}\cos\omega_{\rm out}).$$

Putting $(2/3)(\pi - 2\omega_{\rm in}) \cong \varepsilon_{\rm Oct}$, $\cos\omega_{\rm out} = 1/\sqrt{2}$, $e_{\rm in} = 0.95$, we get $\iota = 40^\circ$ or 140°. Thus, the quadrupole and octupole terms in $\mathrm{d}e_{\rm in}/\mathrm{d}t$ may cancel each other at our resonance region and lead to a major increase in $\mathrm{d}\iota/\mathrm{d}e_{\rm in}$. The resonance at $\iota = 140^\circ$ is important since it shifts the system in phase space to regions of greater instability and greater $Q_{\rm max}$, while the resonance $\iota = 40^\circ$ has rather the opposite effect, if any at all.

Actually, the high inner eccentricity may lead to the formation of close binary stars and ultimately to stellar mergers (Naoz & Fabrycky 2014). Thus, the resonance may be very important in star cluster simulations, but in a different way from the point-mass N-body model. Two ways of defining instability have been used: (1) dynamical instability via escape and (2) collision instability. In Fig. 8, we have considered eccentricity $e_{\rm in} = 0.99$ as leading to a collision and have defined the stability limit $Q_{\rm max}$ such that no collisions occur if we start with $Q > Q_{\rm max}$. We see that for the starting value of the inner eccentricity $e_{\rm in} < 0.6$, the $Q_{\rm max}$ value is not increased by this extra requirement. For larger $e_{\rm in}$ we start getting collisions even though the system would otherwise be stable. This leads to the rapid divergence of the two lines at large $e_{\rm in}$. Actually, by this definition $Q_{max} \to \infty$ when $e_{\rm in} \to 0.99$.

5 SOLUTIONS IN THE COS $\iota_{\rm TOT}$–$e_{\rm IN}$ PLANE

We may illustrate the orbital evolution by solving the Kozai–Lidov octupole equations A1–A7 (Liu at al. 2015) simultaneously (equation A1 for $\mathrm{d}e_{\rm in}/\mathrm{d}t$ was given above).

Fig. 9 shows the evolution in the $\cos\iota_{\rm tot}$–$e_{\rm in}$ plane (where $\iota_{\rm tot}$ is the mutual inclination) with initial mutual inclination $\iota_{\rm tot} = 40^\circ$ and zero octupole momentum ($m_1 = m_2$). The red line corresponds to the exact numerical solution of equations A1–A7 (Liu at al. 2015) and the blue line corresponds to the numerical simulation using symplectic method (Mikkola 1997).

When the octupole momentum is non-zero ($m_1 \neq m_2$), we find a weak resonance without large variations of $\iota_{\rm tot}$ and $e_{\rm in}$. This case is illustrated on the Fig. 10.

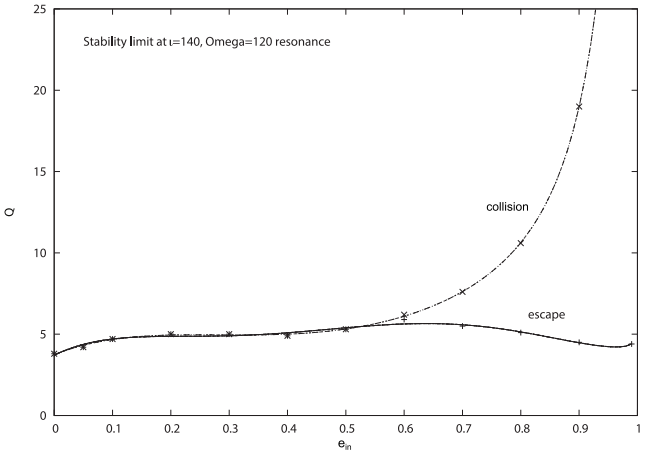

Figure 8. Collision instability illustration for $e_{\rm in}$ up to 0.99. The value of $e_{\rm out}$ used is $e_{\rm out} = 0.5$.

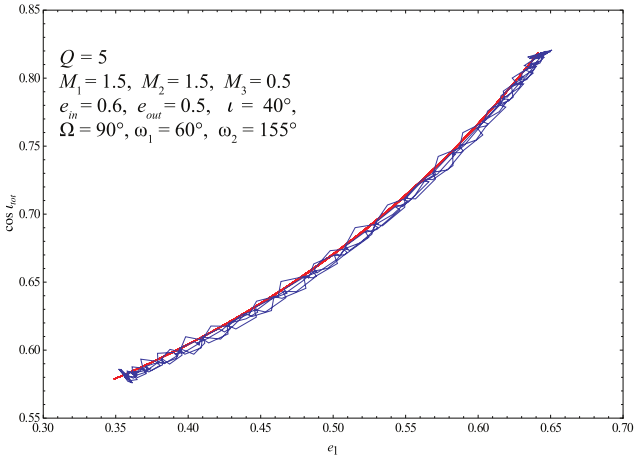

Figure 9. Numerical simulations (blue) and solution of the Kozai–Lidov octupole equations (red) for the zero octupole momentum ($m_1 = m_2$) and $\iota_{\rm tot} = 40^\circ$.

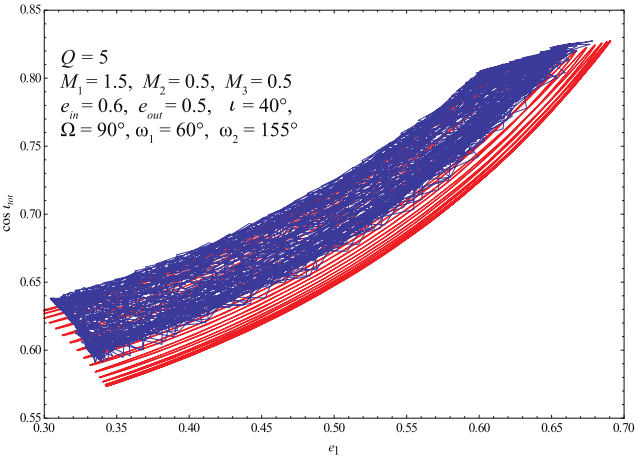

Figure 10. Numerical simulations (blue) and solution of the Kozai–Lidov octupole equations (red) for the non-zero octupole momentum ($m_1 \neq m_2$) and $\iota_{\rm tot} = 40^\circ$.

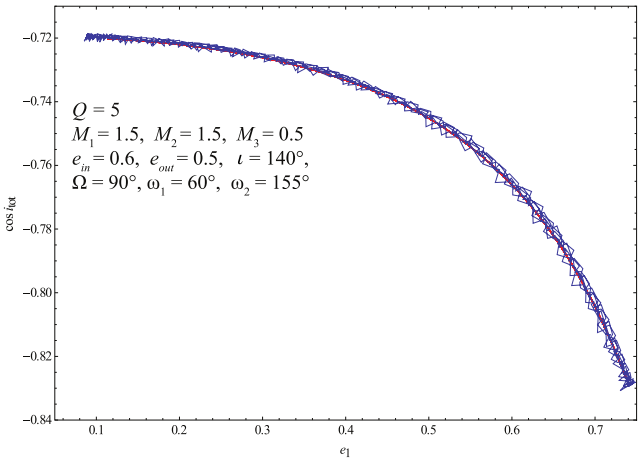

Figure 11. Numerical simulations (blue) and solution of the Kozai–Lidov octupole equations (red) for the zero octupole momentum ($m_1 = m_2$) and $\iota_{\rm tot} = 140^\circ$.

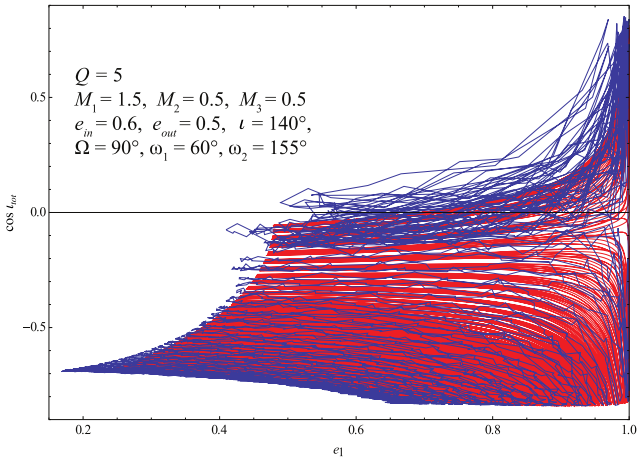

Figure 12. Numerical simulations (blue) and solution of the Kozai–Lidov octupole equations (red) for the case with the inclination flip – non-zero octupole momentum ($m_1 \neq m_2$) and $\iota_{\rm tot} = 140^\circ$.

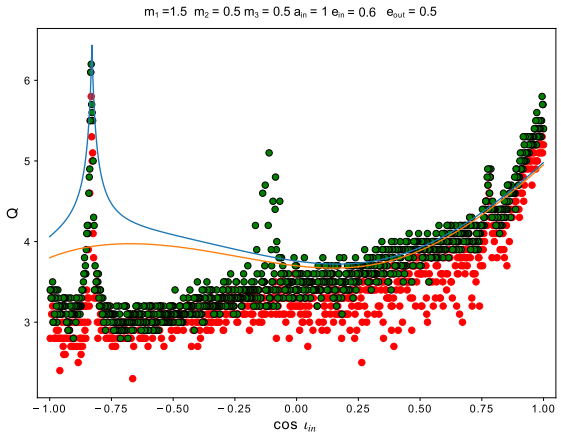

Figure 13. The combined function from Paper I (orange line) and the additional peak (blue line) combine to outline the stability limit in our experiments with $e > 0.5$ ($m_1 = 1.5\,{\rm M}_\odot, m_2 = m_3 = 0.5\,{\rm M}_\odot, a_{\rm in} = 1$ au, $e_{\rm in} = 0.8, e_{\rm out} = 0.5; 75^\circ < \Omega < 105^\circ$).

A completely different picture emerges in the same conditions but at the initial inclination $\iota_{\rm tot} = 140^\circ$. When the octupole momentum is zero ($m_1 = m_2$), the behaviour of the system (Fig. 11) is similar to the case of Fig. 9.

But when the octupole momentum is non-zero ($m_1 \neq m_2$), we have a wide range in the $\iota_{\rm tot}$ and $e_{\rm in}$ variations (Fig. 12) because the inner inclination flips over to the retrograde side from the initial $\iota_{\rm in} = 0$ while the outer inclination remains not too far from its initial value $\iota_{\rm out} \simeq 140^\circ$.

The two considered cases are very close to the octupole-level stationary points $\mathcal{P}_Q^+$, and $\mathcal{P}_Q^-$ studied in the work Hansen & Naoz (2020) for the planetary approximation (m_1, $m_2 \ll m_3$). Although in our case, all three masses are of the same order, the octupole equations mentioned above show good applicability to the analysis of this case.

6 APPROXIMATE EXPRESSION FOR THE RESONANCE

Figures show the $Q_{\rm max}$ value as a function of ι and Ω. The upper level of the instability layer (Paper I) is shown, and normally $Q_{\rm max}$ would not be expected to rise above this level. However, we see that there are higher peaks at certain values of Ω, in a doubly periodic manner, as expected. Overall, the resonance peak is narrow, and the probability of the system falling into this category is quite low. However, we may extend the stability boundary layer in this region by superimposing a Gaussian function on top of it:

$$Q_{\rm max} = a[b + |(\cos\iota - \cos\iota_0)|],$$

where

$$\begin{aligned} \cos\iota_0 &= -0.775, \\ a &= 0.05 \\ b &= 0.02. \end{aligned}$$

Fig. 13 shows how the combined function from Paper I (orange line) and the additional peak (blue line) combine to outline the stability limit in our experiments with $e_{\rm in} > 0.5$. The basic stability line is drawn for $e_{\rm in} = 0.8$, in the middle of the range of the experimental values. $Q_{\rm min}$ and $Q_{\rm max}$ values were calculated for Ω ranging from 75° to 105°.

The red dots mark the $Q_{\rm min}$ value, below which there is no stable configuration. Green dots indicate $Q_{\rm max}$, above which there is no unstable configuration. In the interval Q between the marked green and red points, both stable and unstable configurations can occur.

We also have an unexplained small additional peak of instability in the region of $\cos\iota = -0.12$ ($\iota = 97^\circ$), which does not depend on Ω (longitude of ascending node of the outer orbit). In Figs 3–5, it stands out as a small 'straight ridge'. The investigations of this type of instability should be a topic for future work.

7 SUMMARY

We find that the $\iota = 140^\circ$ resonance has a doubly periodic structure in Ω. This is expected, as the size of the energy change in a single encounter depends on the orbital phase with respect to the 2Ω angle. Subsequently, the orbits will evolve under the Kozai–Lidov octupole resonance, which will affect $e_{\rm in}$ and $\cos\iota$ to a large extent. The study of the individual resonance orbits shows that they arise from an inclination flip. However, the flip requires a pure Newtonian force law and point-like particles, since the inner eccentricity comes extremely close to unity at these times. In the case of stars of finite radii, the flip

is unlikely (Liu at al. 2015) and may lead to the formation of close binary stars and ultimately to stellar mergers (Naoz & Fabrycky 2014). Thus, the resonance may be very important in star cluster simulations, but in a different way from the point-mass *N*-body model.

We have also studied the prominence of resonance as a function of inclination. We suggest a simple formula that predicts the stability limit at the resonance.

DATA AVAILABILITY

The data underlying this article will be shared on reasonable request to the corresponding author.

REFERENCES

Aarseth S. J., Zare K., 1974, Cel. Mech., 10, 185
Aarseth S. J., 2003, Gravitational N-body Simulations: Tools and Algorithms. Cambridge Univ. Press, Cambridge
Benest D., 1989, A&A, 223, 361
Benest D., 1988, A&A, 206, 143
Donnison J. R., 1984, MNRAS, 210, 915
Donnison J. R., 1988, MNRAS, 231, 85
Donnison J. R., Mikulskis D. F., 1992, MNRAS, 254, 21
Donnison J. R., Mikulskis D. F., 1994, MNRAS, 266, 25
Dvorak R., 1986, A&A, 167, 379
Dvorak R., Froeschle C., Froeschle Ch., 1989, A&A, 226, 335
Eggleton P., Kiseleva L., 1995, ApJ, 455, 640
Fehlberg E., 1969, July, 1, Low-order classical Runge-Kutta formulas with step size control and their application to some heat transfer problems. NASA Technical Report 315
Ford E. B., Kozinsky B., Rasio F. A., 2000, ApJ, 535, 385
Georgakarakos N., 2008, Celest. Mech. Dyn. Astron., 100, 151
Graziani F., Black C. D., 1981, ApJ, 251, 337
Hansen B. M. S., Naoz S., 2020, MNRAS, 499, 1682
Harrington R. S., 1968, AJ, 73, 190
Harrington R. S., 1969, Celest. Mech., 1, 200
Harrington R. S., 1972, Celest. Mech., 6, 322
Harrington R. S., 1975, AJ, 80, 1081
Harrington R. S., 1977, AJ, 82, 753
Heggie D. C., 2006, in Flynn C., ed., Few Body Problem, Ann. Univ. Turkuensis, Finland, p. 20
Heggie D. C., Hut P., 2003, The Gravitational Million-Body Problem: a Multidisciplinary Approach to Star Cluster Dynamics. Cambridge Univ. Press, Cambridge
Holman M. J., Wiegert P. A., 1999, AJ, 117, 621
Huang T. Y., Innanen K. A., 1983, AJ, 88, 1064
Kozai Y., 1962, AJ, 67, 591
Krymolowski Y., Mazeh T., 1999, MNRAS, 304, 720
Lidov M. L., 1962, Planet.Space Sci., 9, 719
Lithwick Y., Naoz S., 2011, ApJ, 742, 94
Liu B., Munoz D. J., Lai D., 2015, MNRAS, 447, 747
Marchal C., 1990, The Three-Body Problem. Elsevier, Amsterdam
Mardling R., 2008, in Dynamical Evolution of Dense Stellar Systems. Vesperini E., Giersz M., Sills A., eds., Proc. IAU Symp, 246, IAU Symposium, p. 199
Mardling R., Aarseth S., 1999, in Steves Bonnie A., Roy Archie E., eds. The Dynamics of Small Bodies in the Solar System, Springer Science+Business Media Dordrecht
Mardling R., Aarseth S. J., 2001, MNRAS, 321, 398
Mazeh T., Shaham J., 1979, A&A, 77, 145
Mikkola S., 1997, Celest. Mech. Dyn. Astron., 67, 145
Mylläri A., Valtonen M. J., Pasechnik A., Mikkola S., 2018, MNRAS, 476, 830
Nacozy P. E., 1976, AJ, 81, 787
Naoz S., Fabrycky D. C., 2014, ApJ, 793, 137
Naoz S., Farr W. M., Lithwick Y., Rasio F. A., Teyssandier J., 2013, MNRAS, 431, 2155
Pendleton Y. J., Black D. C., 1983, AJ, 88, 1415
Pilat-Lohinger E., Funk B., Dvorak R., 2003, A&A, 400, 1085
Rabl G., Dvorak R., 1988, A&A, 191, 385
Roy A., Haddow M., 2003, Celest. Mech. Dyn. Astron., 87, 411
Roy A. E., Walker I. W., Carusi A., Valsecchi G. B., 1984, A&A, 141, 25
Söderhjelm S., 1984, A&A, 141, 232
Szebehely V., 1976, Celest. Mech., 15, 107
Szebehely V., McKenzie R., 1977, AJ, 82, 303
Szebehely V., Zare K., 1977, A&A, 58, 145
Valtonen M., Karttunen H., 2006, The Three-Body Problem. Cambridge Univ. Press, Cambridge
Valtonen M., Mylläri A., Orlov V., Rubinov A., 2008, in Dynamical Evolution of Dense Stellar Systems. Vesperini E., Giersz M., Sills A., eds., Proc. IAU Symp., 246, International Astronomical Union, IAU Symposium, p. 209
Walker I. W., Roy A. E., 1981, CeM, 24, 195
Walker I. W., Roy A. E., 1983, CeM, 29, 117
Zhang E., Naoz S., Will C. M., 2023, ApJ, 952, 103

This paper has been typeset from a TEX/LATEX file prepared by the author.